Contents lists available at ScienceDirect

Tetrahedron

journal homepage: www.elsevier.com/locate/tet

Acyl radical addition to benzene and related systems—a computational study

Ruth I.J. Amos [a,b], Jason A. Smith [a,b], Brian F. Yates [a,b], Carl H. Schiesser [a,c,d,*]

[a] ARC Centre of Excellence for Free Radical Chemistry and Biotechnology, Australia
[b] School of Chemistry, University of Tasmania, Private Bag 75, Hobart, Tasmania 7001, Australia
[c] School of Chemistry, The University of Melbourne, Victoria 3010, Australia
[d] Bio21 Molecular Science and Biotechnology Institute, The University of Melbourne, Victoria 3010, Australia

ARTICLE INFO

ABSTRACT

The addition of the acetyl radical to benzene, aniline, trifluoromethylbenzene and naphthalene has been investigated using DFT calculations. Addition to benzene is calculated to have an energy barrier of 63.6 kJ mol^{-1} at the BHandHLYP/6-311G(d,p)+ZPE level of theory. This reaction is associated with simultaneous SOMO→π* and π→SOMO interactions with the latter interaction dominating, suggesting that acetyl reacts predominantly as an electrophilic radical in its interaction with benzene. Addition to the *ortho* and *para* positions of aniline is calculated to be slightly less favourable, while attack at the *meta* position is predicted to be unaffected in relation to the chemistry involving benzene. Inclusion of the electron-withdrawing substituent, trifluoromethyl, is predicted to accelerate reactions slightly at the *ortho* and *para* positions, while attack at the C1 position of naphthalene is calculated to involve a barrier of 50.3 kJ mol^{-1} (BHandHLYP/6-311G(d,p)+ZPE).

1. Introduction

The formation of carbon–carbon bonds is integral to organic chemistry and the use of free radicals in synthesis is now accepted as key methodology, that is, particularly useful for preparing rings through homolytic addition to carbon–carbon double bonds. While alkyl radicals have been extensively explored in this regard,[1–4] acyl radicals are especially useful as cyclisation reactions result in functionalized ring systems that include cyclic ketones, lactones and lactams.[5–11] An example of this chemistry is depicted in Scheme 1.[12]

Scheme 1.

While acyl radicals can be generated readily from seleno-[13] or telluro-esters,[6,14] the use of the free radical carbonylation methodology developed by Ryu and co-workers offers a convenient

alternative starting from the usual suite of precursors, an example of which is provided in Scheme 2.[10,11,15]
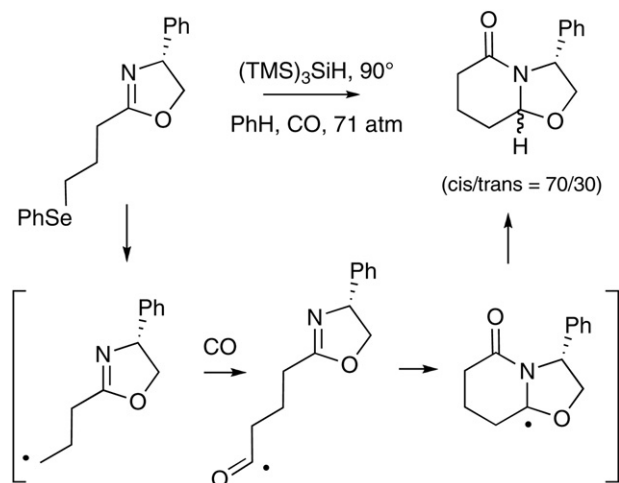
Scheme 2.

While acyl radicals have generally been viewed as being nucleophilic,[5,16–18] Ryu recently showed that these radicals are *N*-philic and prefer to attack at the electron rich nitrogen end of C=N bonds,[5] often defying the usual selectivity rules.[19–21] *Ab initio* and density

* Corresponding author. Tel.: +61 3 8344 2432; fax: +61 3 9347 8189; e-mail address: carlhs@unimelb.edu.au (C.H. Schiesser).

functional techniques have been used to provide an understanding of the mechanism for homolytic addition by these and related radicals at imines, hydrazones and related systems.[22–25] These studies have shown that while acyl radicals are electrophilic or nucleophilic radicals depending on the reacting partner, they can 'masquerade' as electrophiles and accept an electron pair in the presence of suitable electron-rich systems.[26,27]

As part of an ongoing study, we now report the results of a computational investigation into the reaction of the acetyl radical with benzene and substituted benzenes with varying electron demand.

2. Computational methods

Geometry optimizations for the stationary points involved in the reaction of acetyl radical with benzene were performed using the 6-311G(d,p) basis set at the HF, B3LYP and BHandHLYP levels of theory, with higher-level single-point calculations performed at QCISD/6-311G(d,p), CCSD(T)/6-311G(d,p) and CCSD(T)/6-311+G (d,p) on BHandHLYP/6-311G(d,p) optimized geometries. This study (*vide supra*), as well as previous benchmarking studies[22,23,25,27] have established that the BHandHLYP/6-311G(d,p) is a reliable level of theory for the study of the reactions of acyl and related radicals with a variety of π-systems. Consequently, geometry optimizations were performed for the majority of systems in this study using the Gaussian 03 program[28] using that level of theory. Unrestricted methods (UHF, UB3LYP, UBH and HLYP) were used for open-shell systems. All optimized stationary points were verified as corresponding to ground or transition state structures using vibrational frequency analysis. Zero-point vibrational energy (ZPE) corrections have been applied to all structures. Natural Bond Orbital (NBO) analyses were carried out using the NBO 5.0[29] software linked through the Gaussian 03 program.

Optimized geometries and energies for all transition structures are available as Supplementary data.

3. Results and discussion

3.1. Reaction of the acetyl radical with benzene and naphthalene

We began our study by examining the potential energy surface for the addition of the acetyl radical to benzene. Table 1 lists the calculated energy barriers at the levels of theory employed in this

Table 1
Calculated energy barriers[a] and transition state frequencies[b] for the reaction of acetyl radical with substituted benzenes (**1**) and naphthalene (Scheme 3)

Transition state	Level of theory	ΔE_1^a	ΔE_1^a+ZPE	ΔE_2^a	ΔE_2^a+ZPE	ν_{TS}
2 (R=H)	HF/6-311G(d,p)	60.6	55.4	78.9	87.0	513i
	B3LYP/6-311G(d,p)	53.7	54.3	46.3	41.9	417i
	BHandHLYP/6-311G(d,p)	63.6	63.6	70.4	65.6	514i
	QCISD/6-311G(d,p)[c]	62.0	—	79.1	—	—
	CCSD(T)/6-311G(d,p)[d]	56.6	—	68.1	—	—
	CCSD(T)/6-311+G(d,p)[e]	54.2	—	67.8	—	—
3	BHandHLYP/6-311G(d,p)	50.8	50.3	91.6	85.3	486i
4	BHandHLYP/6-311G(d,p)	57.1	56.5	78.3	72.2	487i
2 (R=o-NH₂)	BHandHLYP/6-311G(d,p)	65.3	64.8	85.3	78.1	578i
2 (R=m-NH₂)	BHandHLYP/6-311G(d,p)	63.1	63.1	69.7	65.0	511i
2 (R=p-NH₂)	BHandHLYP/6-311G(d,p)	71.3	69.6	75.8	70.2	565i
2 (R=o-CF₃)	BHandHLYP/6-311G(d,p)	58.5	58.9	73.0	66.9	461i
2 (R=m-CF₃)	BHandHLYP/6-311G(d,p)	62.0	61.9	66.2	61.4	487i
2 (R=p-CF₃)	BHandHLYP/6-311G(d,p)	58.2	58.6	71.9	66.5	473i

[a] Energies in kJ mol⁻¹. ΔE_1^a and ΔE_2^a are the 'forward' and 'reverse' energy barriers as depicted in Scheme 2.
[b] Frequencies in cm⁻¹.
[c] QCISD/6-311G(d,p)//BHandHLYP/6-311G(d,p).
[d] CCSD(T)/6-311G(d,p)//BHandHLYP/6-311G(d,p).
[e] CCSD(T)/6-311+G(d,p)//BHandHLYP/6-311G(d,p).

study for the homolytic addition of the acetyl radical to benzene (**1**, R=H) according to the reaction shown in Scheme 3. The barrier ($\Delta E_1^\ddagger$) for the forward reaction is predicted to be in the range of 52–64 kJ mol⁻¹ depending on the level of theory. Except at the B3LYP/6-311G(d,p) level, the overall process is predicted to be slightly exothermic ($\Delta E_2^\ddagger$=65–88 kJ mol⁻¹). On the basis of the data provided in Table 1, we are confident that the BHandHLYP/6-311G (d,p) is a reliable DFT level of theory for the study of the reactions in this work as it provides energy data for $\Delta E_1^\ddagger$ and $\Delta E_2^\ddagger$ most consistent with the highest (CCSD(T)) level of theory. This observation is in agreement with our earlier reports.[22,23,25,27]
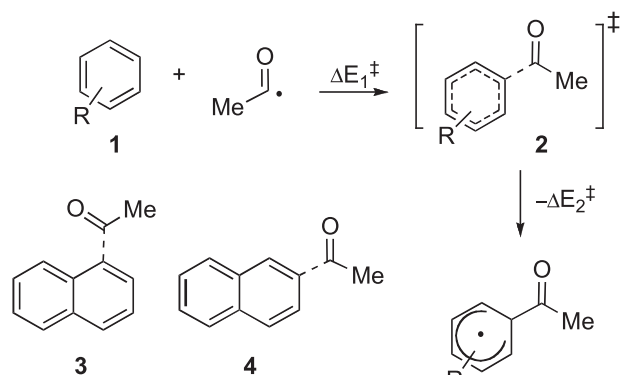
Scheme 3.

Figure 1 depicts the structure of the transition state (**2**, R=H) for the addition of the acetyl radical to benzene calculated at the BHandHLYP/6-311G(d,p) level of theory. Inspection of Figure 1 reveals a distance in the transition state of 2.089 Å associated with the attack trajectory, with a corresponding angle of 116.3°. These data are to be compared with similar data obtained for the addition of acetyl radical to pyridine where transition state separations of between 2.114 and 2.215 Å were obtained at the same level of theory, depending on the position of attack. Structural details for **2** at the remaining levels of theory can be found in the Supplementary data.
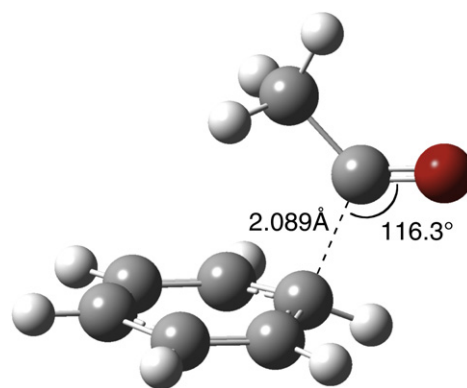

Figure 1. BHandHLYP/6-311G(d,p) optimized structure for the transition state (**2**) involved in the reaction of acetyl radical with benzene.

NBO analysis of transition state **2** (R=H) reveals a SOMO$_{radical}$→π*$_{aromatic}$ interaction worth 273 kJ mol⁻¹ evident in the α spin set, and a π$_{aromatic}$→ SOMO$_{radical}$ interaction worth 383 kJ mol⁻¹ in the β spin set. These interactions are depicted in Figure 2 and listed in Table 2 (together with others calculated as part of this study) and indicate that the acetyl radical is acting essentially as an ambiphilic radical in its reaction with benzene, with about 58% electrophilic and 42% nucleophilic components to the overall transition state interaction energy.
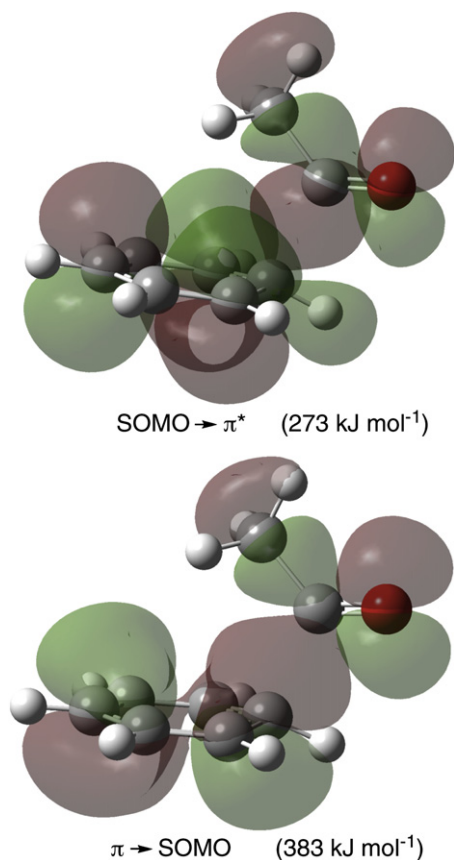
Figure 2. Key BHandHLYP/6-311G(d,p) generated molecular orbitals involved in the homolytic addition of acetyl radical to benzene.

Table 2
BHandHLYP/6-311G(d,p) calculated NBO orbital interaction energies[a] in transition states **2** and **4**

Transition state	SOMO→π*	π→SOMO
2 (R=H)	273	383
3	219	261
4	272	304
2 (R=o-NH$_2$)	231	399
2 (R=m-NH$_2$)	303	324
2 (R=p-NH$_2$)	262	398
2 (R=o-CF$_3$)	295	262
2 (R=m-CF$_3$)	289	324
2 (R=p-CF$_3$)	269	334

[a] Energies in KJ mol^{-1}.

The reaction of an acetyl radical with naphthalene is calculated to be more favourable than the corresponding reaction with benzene, with BHandHLYP/6-311G(d,p) calculated energy barriers ($\Delta E_1^\ddagger$) of about 50 and 57 kJ mol^{-1} (ZPE included) for attack at the C1 and C2 positions, respectively. In addition, these reactions are also calculated to be more exothermic, with energy barriers ($\Delta E_2^\ddagger$) for the fragmentation of the adduct radical of 85 and 72 kJ mol^{-1} (ZPE included) (Table 1). This is not surprising given the inherent aromaticity differences between the two molecules.[30]

Figure 3 depicts the structures of transition states (**3**, **4**) for the addition of an acetyl radical to the C1 and C2 positions of naphthalene, respectively. Inspection of Figure 3 reveals a transition state separation of 2.129–2.164 Å, with corresponding angles of 116–117°. NBO analysis of transition states **3** and **4** reveals that the acetyl radical also reacts predominantly as an ambiphilic radical at both positions of naphthalene, but the contribution of the
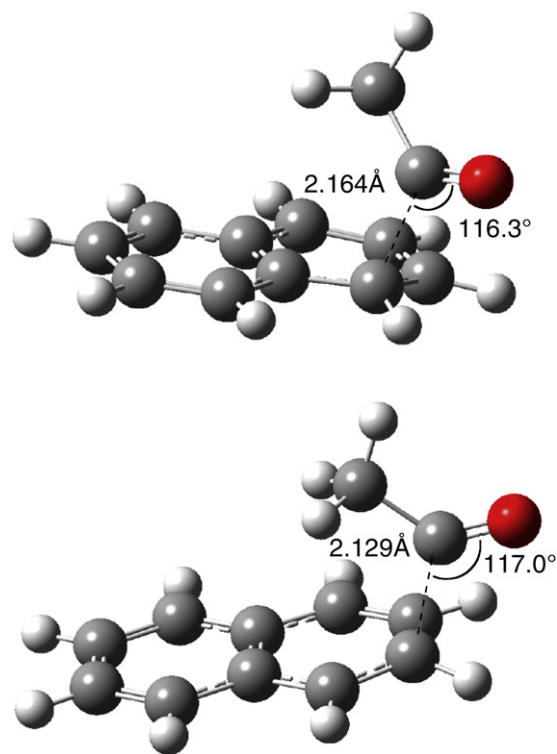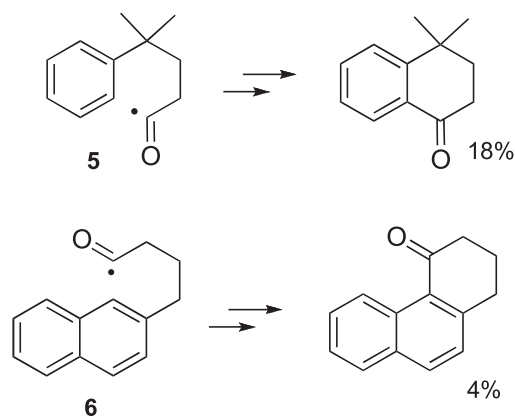

Figure 3. BHandHLYP/6-311G(d,p) optimized structures for the transition states **3** (above) and **4** (below) involved in the reaction of acetyl radical with naphthalene.

π→SOMO interaction is somewhat less (52–54%) than that observed in the case of benzene (Table 2).

We are only aware of one example in which an acyl radical undergoes homolytic addition to a benzene ring (**5**), and one example involving a naphthalene ring (**6**) (Scheme 4); both transformations proceed in low yield.[31,32] Consistent with this, BHandHLYP/6-311G(d,p)+ZPE calculations predict that the ring-closure of **5** proceeds with an energy barrier of about 54 kJ mol^{-1}, and is exothermic by 22 kJ mol^{-1}; the transition structure (**7**) involved in the cyclization of **5** is depicted in Figure 4.

Scheme 4.

3.2. Reaction of acetyl radical with aniline and trifluoromethylbenzene

We next chose to explore the effect of electron-donating (NH$_2$) and electron-withdrawing (CF$_3$) substituents on the overall chemistry described above. To that end, the potential energy
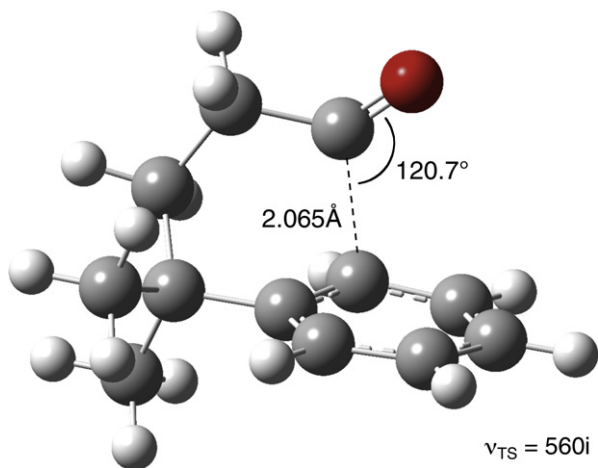
Figure 4. BHandHLYP/6-311G(d,p) optimized structure for the transition state (**7**) involved in the cyclization of radical **5**.

surfaces for the reaction of acetyl radical at the *ortho*, *meta* and *para* positions in aniline and trifluoromethylbenzene were examined. Figure 5 depicts the structures of transition states **2** (R=*p*-NH$_2$, *p*-CF$_3$) for the attack at the *para* positions in both molecules; the remaining structures **2** can be found in Figure S1 of the Supplementary data and are similar to those shown in Figure 3. Inspection of Figure 5 reveals transition state separations and angles similar to those observed for the other transition states in this study (**2**, R=H; **3**, **4**) at about 2.1 Å and 116°, respectively.

Table 1 lists the energy barriers for the forward ($\Delta E_1^{\ddagger}$) and reverse ($\Delta E_2^{\ddagger}$) reactions for attack at each position in both systems (R=NH$_2$, CF$_3$). It is interesting to note that in the case of the electron-rich system, aniline, the energy barriers for the attack at the

ortho and *meta* positions are very similar to that of the parent system, benzene, with attack at the *para* position slightly less favoured by about 7 kJ mol^{-1}. In contrast, the electron-deficient system, trifluoromethylbenzene appears to benefit slightly from inclusion of the withdrawing group at the *ortho* and *para* positions, with barriers ($\Delta E_1^{\ddagger}$) for the forward reaction some 5 kJ mol^{-1} lower than that for the reaction with benzene itself. Once again, the *meta* position is unaffected.

Not surprisingly, the data in Table 2 reveal that acetyl is a more electrophilic radical when it reacts at the *ortho* and *para* positions in aniline than in its reaction with benzene, while in its reaction with the electron-deficient system (R=CF$_3$), acetyl begins to prefer to react in a slightly nucleophilic manner at the *ortho* position, with E(SOMO→π$_*$)>E(π→SOMO). Despite these trends, acetyl is still predominantly ambiphilic in nature towards the substituted benzenes in this study.

As we have been interested in multi-component orbital interactions during reactions involving acyl and related radicals,[10,16,22–25,33–35] we were keen to observe such interactions in the chemistry discussed above. NBO analysis at the BHandHLYP/6-311G(d,p) level of theory of each transition state (**2**–**4**) failed to locate the typical π$_{aromatic}$→π$_{*acyl}$ or LP→π$_{*acyl}$ interaction usually observed when the acetyl radical masquerades as an electrophile. It should be noted this interaction is observed when the acetyl radical reacts with aminoethylene;[22] the lack of this interaction in the reaction involving aniline is attributed to the aromatic nature of the π-systems undergoing reaction.

4. Conclusion

The acetyl radical is calculated to react as an ambiphilic radical in its reactions with benzene, naphthalene, aniline and trifluoromethylbenzene. Energy barriers for homolytic addition range from 50.3 kJ mol^{-1} for attack at C1 of naphthalene, to 69.6 kJ mol^{-1} for attack at the *para* position in aniline. NBO analysis reveals that the acetyl radical is most electrophilic (63%) in its reaction at the *ortho* position in aniline, and least (47%) in its reaction at the *ortho* position in trifluoromethylbenzene, compared with benzene (58%). Somewhat surprisingly, in none of the reactions in this study did NBO analysis reveal any multi-component orbital interactions.

Supplementary data

The following are available as Supplementary data: Figure S1; optimized geometries (Gaussian archive entries) of structures **2**–**4**, **7**. Supplementary data associated with this article can be found in online version at doi:10.1016/j.tet.2010.07.041.
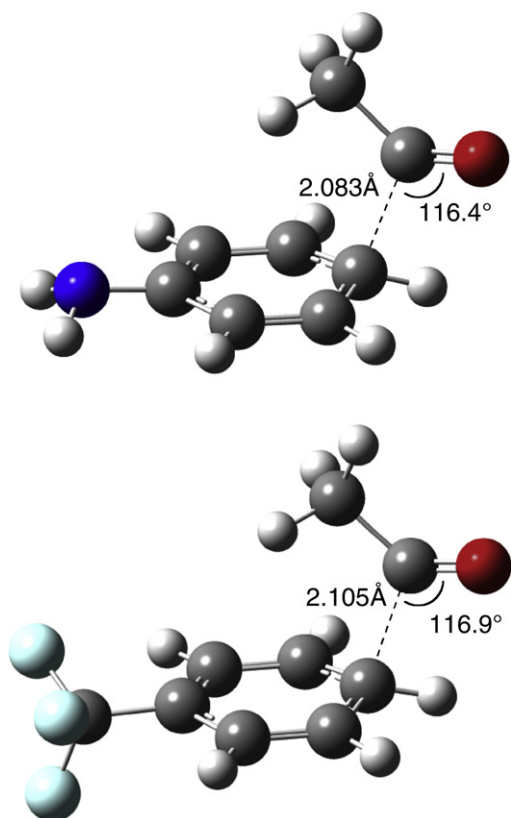

Figure 5. BHandHLYP/6-311G(d,p) optimized structures for the transition states **2**, R=*p*-NH2 (above) and R=*p*-CF3 (below) involved in the reaction of acetyl radical with aniline and trifluoromethylbenzene.

References and notes

1. Hart, D. J. *Science* **1984**, *223*, 883–887.
2. Ramaiah, M. *Tetrahedron* **1987**, *43*, 3541–3676.
3. Curran, D. P. *Synthesis* **1988**, 417–439.
4. Curran, D. P. *Synthesis* **1988**, 489–513.
5. Chatgilialoglu, C.; Crich, D.; Komatsu, M.; Ryu, I. *Chem. Rev.* **1999**, *99*, 1991–2069.
6. Crich, D.; Chen, C.; Hwang, J. –T.; Yuan, H.; Papadatos, A.; Walter, R. I. *J. Am. Chem. Soc.* **1994**, *116*, 8937–8951.
7. Crich, D.; Quintero, L. *Chem. Rev.* **1989**, *89*, 1413–1432.

8. Mendenhall, G. D.; Protasiewicz, J. D.; Brown, C. E.; Ingold, K. U.; Lusztyk, J. *J. Am. Chem. Soc.* **1994**, *116*, 1718–1724.
9. Mendenhall, G. G.; Protasiewicz, J. D.; Brown, C. E.; Ingold, K. U.; Lusztyk, J. *J. Am. Chem. Soc.* **1994**, *116*, 5525.
10. Schiesser, C. H.; Wille, U.; Matsubara, H.; Ryu, I. *Acc. Chem. Res.* **2007**, *40*, 303–313.
11. Ryu, I.; Miyazato, H.; Kuriyama, H.; Matsu, K.; Tojino, M.; Fukuyama, T.; Minakata, S.; Komatsu, M. *J. Am. Chem. Soc.* **2003**, *125*, 5632–5633.
12. Boger, D. L.; Mathvink, R. J. *J. Org. Chem.* **1992**, *57*, 1429–1443.
13. Pfenninger, J.; Heuberger, C.; Graf, W. *Helv. Chim. Acta* **1980**, *63*, 2328–2337.
14. Chen, C.; Crich, D.; Papadatos, A. *J. Am. Chem. Soc.* **1992**, *114*, 8313–8314.
15. Ryu, I.; Yamazaki, H.; Ogawa, A.; Kambe, N.; Sonoda, N. *J. Am. Chem. Soc.* **1993**, *115*, 1187–1189.
16. Matsubara, H.; Falzon, C. T.; Ryu, I.; Schiesser, C. H. *Org. Biomol. Chem.* **2006**, *4*, 1920–1926.
17. Bellatti, M.; Caronna, T.; Citterieo, A.; Minisci, F. *J. Chem. Soc., Perkin Trans. 2* **1976**, 1835–1838.
18. Caronna, T.; Citterio, A.; Bellatti, M. *J. Chem. Soc., Chem. Commun.* **1976**, 987–988.
19. Baldwin, J. E. *J. Chem. Soc., Chem. Commun.* **1976**, 734–746.
20. Beckwith, A. L. J.; Schiesser, C. H. *Tetrahedron* **1985**, *41*, 3925–3941.
21. Spellmeyer, D. C.; Houk, K. N. *J. Org. Chem.* **1987**, *52*, 959–974.
22. Kyne, S. H.; Schiesser, C. H.; Matsubara, H. *J. Org. Chem.* **2008**, *73*, 427–434.
23. Kyne, S. H.; Schiesser, C. H. *Aust. J. Chem.* **2009**, *62*, 728–733.
24. Amos, R. I. J.; Smith, J. A.; Yates, B. F.; Schiesser, C. H. *Tetrahedron* **2009**, *65*, 7653–7657.
25. Kyne, S. H.; Schiesser, C. H.; Matsubara, H. *Org. Biomol. Chem.* **2007**, *5*, 3938–3943.
26. Falzon, C. T.; Ryu, I.; Schiesser, C. H. *Chem. Commun.* **2002**, 2338–2339.
27. Schiesser, C. H.; Matsubara, H.; Ritsner, I.; Wille, U. *Chem. Commun.* **2006**, 1067–1069.
28. Frisch, M. J.; Trucks, G. W.; Schlegel, H. B.; Scuseria, G. E.; Robb, M. A.; Cheeseman, J. R.; Montgomery, J. A., Jr.; Vreven, T.; Kudin, K. N.; Burant, J. C.; Millam, J. M.; Iyengar, S. S.; Tomasi, J.; Barone, V.; Mennucci, B.; Cossi, M.; Scalmani, G.; Rega, N.; Petersson, G. A.; Nakatsuji, H.; Hada, M.; Ehara, M.; Toyota, K.; Fukuda, R.; Hasegawa, J.; Ishida, M.; Nakajima, T.; Honda, Y.; Kitao, O.; Nakai, H.; Klene, M.; Li, X.; Knox, J. E.; Hratchian, H. P.; Cross, J. B.; Bakken, V.; Adamo, C.; Jaramillo, J.; Gomperts, R.; Stratmann, R. E.; Yazyev, O.; Austin, A. J.; Cammi, R.; Pomelli, C.; Ochterski, J. W.; Ayala, P. Y.; Morokuma, K.; Voth, G. A.; Salvador, P.; Dannenberg, J. J.; Zakrzewski, V. G.; Dapprich, S.; Daniels, A. D.; Strain, M. C.; Farkas, O.; Malick, D. K.; Rabuck, A. D.; Raghavachari, K.; Foresman, J. B.; Ortiz, J. V.; Cui, Q.; Baboul, A. G.; Clifford, S.; Cioslowski, J.; Stefanov, B. B.; Liu, G.; Liashenko, A.; Piskorz, P.; Komaromi, I.; Martin, R. L; Fox, D. J.; Keith, T.; Al-Laham, M. A.; Peng, C. Y.; Nanayakkara, A.; Challacombe, M.; Gill, P. M. W.; Johnson, B.; Chen, W.; Wong, M. W.; Gonzalez, C.; Pople, J. A. *Gaussian 03, Revision D.01*; Gaussian: Wallingford CT, 2004.
29. Glendening, E. D.; Badenhoop, J. K.; Reed, A. E.; Carpenter, J. E.; Bohmann, J. A.; Morales, C. M.; Weinhold, F. *NBO5.0*; Theoretical Chemistry Institute: University of Wisconsin: Madison, WI, 2001.
30. Mayo, F. R.; Hardy, W. B. *J. Am. Chem. Soc.* **1952**, *74*, 911–917.
31. Urry, W. H.; Trecker, D. J.; Hartzler, H. D. *J. Org. Chem.* **1964**, *29*, 1663–1669.
32. Grissom, J. W.; Klingberg, D.; Meyenburg, S.; Stallman, B. L. *J. Org. Chem.* **1994**, *59*, 7876–7888.
33. Krenske, E. H.; Schiesser, C. H. *Org. Biomol. Chem.* **2008**, *6*, 854–859.
34. Horvat, S. M.; Schiesser, C. H. *Organometallics* **2009**, *28*, 3311–3318.
35. Tran, T. A.; Schiesser, C. H. *Bull. Korean Chem. Soc.* **2010**, *31*, 595–598.